AC Permeability of the Flux-Line Liquid in the Anisotropic High-T_C Superconducting Crystals

Chien-Jang Wu and Tseung-Yuen Tseng, *Senior Member, IEEE*

Abstract— AC properties of the flux-line liquid in the anisotropic high-temperature superconducting crystals in a parallel field are theoretically investigated. The ac responses in the simple flux-flow regime are analyzed from associated effective ac-magnetic permeability calculated on the hydrodynamic theory basis. The responses are studied as functions of anisotropic ratio and sample dimensions. The results illustrate the influence of the platelet crystal's size on permeability in the anisotropic superconductors while in the isotropic superconductors, the relationship of responses between a square rod and cylinder is found. It indicates that the permeability of a cylinder can be essentially replaced by that of a square rod and vice versa. The geometric effect on response is also elucidated in the isotropic superconductors.

I. INTRODUCTION

THE AC TECHNIQUES are extensively used to measure the ac and microwave properties of the high-temperature superconductors (HTSC) in the mixed state. By measuring related quantities, such as surface impedance and magnetic permeability, one can extract some fundamental information which is of vital importance in the understanding of flux-line dynamics. AC measurements are usually conducted by the microwave-surface impedance [1]–[6], vibrating-reed resonator [7], and ac-magnetic permeability [8]. For a linear response study, a small alternating magnetic field is usually superimposed to a large static field, and the response is not a function of amplitude of the ac field. The ac field is applied parallel to the surface of the superconductor, and screening currents are generated near the surface. The currents induce Lorentz forces which will act on the flux lines and cause an oscillation of the flux-line lattice. The oscillation then propagates into the interior of the superconductor due to flux-line interaction. During propagation, the flux lines are impeded by friction together with pinning forces. The ac properties of the flux-line system are therefore strongly related to the nature of flux-line dynamics.

Up to the present, many efforts have been made to theoretically investigate the ac response of a flux-line system in the HTSC. Coffey and Clem [9]–[11] developed a unified theory for the RF-surface impedance and magnetic permeability in the isotropic type-II superconductors. The effects of flux pinning, flux creep, and flow on flux-line dynamics are incorporated

by a self-consistent approach. The phenomenological model has been utilized to investigate the flux-line dynamics from the measurements of surface impedance in YBa$_2$Cu$_3$O$_{7-x}$ (YBCO) thin films [3], [5], [6]. By making use of a continuum description of the flux-line lattice for $B > 2B_{c1}$ (B_{c1} is the lower critical field), Brandt [12] also investigated the linear ac response of the elastically pinned flux-line lattice. Considering all possible effects due to image vortexes, flux pinning, flux flow, flux creep, and nonlocal elasticity, a different ac-complex penetration length λ is also given. The ac-dissipation peak occurs when λ is of the order of the sample size and is commonly ascribed to the skin-size effect [9]–[13].

As is well known, there exists a large flux-liquid region in the (H, T) phase diagram of HTSC. A popular model used in the study of linear ac response of flux-line liquid is the thermally assisted flux-flow (TAFF) theory where the thermally activated depinning of flux lines is incorporated by generalizing the usual Bardeen–Stephen (BS) theory [14]. The TAFF naturally reduces to the BS when temperatures are higher than the typical pinning energy. Van der Beek and Kes have successfully reproduced the irreversibility line of the flux-line liquid within the framework of TAFF [15]. In addition, Yeh [16] generalized the TAFF idea to study the microwave response of HTSC near the depinning threshold. However, the idea of TAFF does not fully describe the flux-line interactions in the flux liquid. It is natural to consider another relevant model to encompass the intervortex interactions together with nonlocality effect arisen from viscous forces. Recently, Chen and Marchetti [17] studied the ac response of flux-line liquid from the viewpoint of hydrodynamics in which the associated intervortex interaction as well as nonlocality effects were incorporated appropriately.

The theoretical treatments described above primarily lie in the investigation of the influence of flux-line dynamics on the ac permeability and surface impedance. This influence is naturally considered to be the intrinsic property of the superconductors. An interesting issue concerning the geometric effect of the ac permeability was recently pointed out by Gough and Exon [4]. The authors stressed the role of the thin edges of a platelet crystal in considering the normal-state microwave response for extremely anisotropic HTSC oriented in a parallel field. In a parallel field configuration, the ac field is applied parallel to the ab-plane, and the electrodynamics of the superconductor are thus strongly anisotropic, especially in the Bi$_2$Sr$_2$CaCu$_2$O$_{8+x}$ (BSCCO) system. As reported in literature, the normal-state anisotropic resistivity ratio, ρ_c/ρ_{ab}, is about 10^5 for this system [18], [19]. The field penetration depth

through thin edges is thus 300 times larger than that of main surfaces. Also, in the mixed state the broadening of resistive transition below T_c is strongly anisotropic [20]. What is more, the flux-line dynamics are closely related to the London penetration depths also shown to be anisotropic in a parallel field configuration. The anisotropic London penetration ratio $\gamma = \lambda_c/\lambda_{ab}$ is reported to be 5–8 for YBCO and 50–250 for BSCCO [21]. With these facts, the effect of thin edges on the mixed-state microwave response is therefore necessary to reconsider. The same issue accompanied by the isotropic platelet crystal is also worthwhile to investigate. As mentioned by Gough and Exon [4], the microwave absorption from thin edges is negligibly small as compared with that from main flat surfaces. However, as will be shown later, this argument appears to be questionable. The dependence of ac permeability on thin edges will be clearly elucidated for both anisotropic and isotropic superconductors. In addition, we shall numerically demonstrate the relationship of permeabilities between the isotropic square rod and cylinder. It is of particular interest to note that ac responses of these two special geometries can be approximately interchanged when the cylinder's radius is equal to a half-width of the square rod.

II. CALCULATION OF DIMENSIONLESS AC PERMEABILITY

Consider a uniaxial type-II superconductor in the shape of a long rectangular rod whose length, width, and thickness are $|y| \leq b$, $|x| \leq a$, $|z| \leq t$, respectively. In HTSC, the c-axis is chosen as the z-axis and the ab-plane as xy-plane. A steady magnetic field $\mathbf{H} = \hat{y}H$ is applied parallel to the four planes at $x = \pm a$ and $z = \pm t$ to produce a uniform flux-line lattice. The densities of vortex n_0 and average flux density $\mathbf{B}_0 = \hat{y}B_0$ are related by $n_0 = B_0/\phi_0$ and $a_0 \approx 1/\sqrt{n_0}$ where ϕ_0 is the flux quantum defined by $\phi_0 = hc/2e$, and a_0 is the intervortex spacing where c is the speed of light, e the electronic charge, and h the Planck constant (the Gaussian unit is used). We assume that the length is much larger than the thickness. This assumption permits us to ignore the demagnetizing field, and the average flux density is approximated as H, namely $B_0 \approx H$. In this paper, we are concerned with the regime $H_{c1} \ll B_0 \ll H_{c2}$ i.e., $\xi_{ab} \ll a_0 \ll \lambda_{ab}$, where ξ_{ab} and λ_{ab} are the coherence and penetration lengths in the ab-plane, respectively. The flux-line lattice is considered to be in a liquid phase, and the vortex dynamics are described by some hydrodynamic fields coarse-grained over several lattice spacings.

The electrodynamics of the flux-line liquid in a superconductor are described by Maxwell's equations

$$\nabla \times \mathbf{e} = -\frac{1}{c}\frac{\partial \mathbf{b}}{\partial t} \qquad (1)$$

$$\nabla \times \mathbf{b} = \frac{4\pi}{c}\mathbf{j} + \frac{1}{c}\frac{\partial \mathbf{e}}{\partial t} \qquad (2)$$

$$\nabla \cdot \mathbf{e} = 4\pi\rho \qquad (3)$$

$$\nabla \cdot \mathbf{b} = 0 \qquad (4)$$

a two-fluid equation

$$\mathbf{j} = \mathbf{j_n} + \mathbf{j_s} \qquad (5)$$

and the London equation in the presence of vortices [17]

$$\nabla \times \mathbf{\Lambda} \cdot \mathbf{j_s} = \frac{c}{4\pi}(-\mathbf{b} + \phi_0 \mathbf{T}) \qquad (6)$$

where e and b are the local fields, $\mathbf{j_s}$ the supercurrent density (the normal current density $\mathbf{j_n}$ is related by $\mathbf{j_n} = \sigma_n \mathbf{e}$ with conductivity tensor σ_n for normal electrons), $\mathbf{\Lambda}$ is the diagonal tensor with entities $\Lambda_{xx} = \Lambda_{yy} = \lambda_{ab}^2$ and $\Lambda_{zz} = \lambda_c^2$, and $\mathbf{T}$ is defined by $\mathbf{T} = \hat{z}n + \tau$ with n and τ being the coarse-grained hydrodynamic density and tilt fields of the flux-line lattice. By making use of (1)–(6), we have

$$\nabla \times \mathbf{\Lambda} \cdot \nabla \times \mathbf{b} + \mathbf{b} = \phi_0 \mathbf{T} + \frac{4\pi}{c}\nabla \times (\mathbf{\Lambda} \cdot \mathbf{j_n})$$
$$+ \frac{1}{c}\nabla \times \left(\mathbf{\Lambda} \cdot \frac{\partial \mathbf{e}}{\partial t}\right). \qquad (7)$$

Equation (7) can be further explicitly expressed in terms of components of the conductivity tensor. The result is

$$\nabla \times \mathbf{\Lambda} \times \mathbf{b} + \mathbf{b}$$
$$= \phi_0 \mathbf{T} - \frac{4\pi}{c^2}\sigma_{nab}\lambda^2 \frac{\partial \mathbf{b}}{\partial t} + \frac{4\pi}{c}(\sigma_{nc}\lambda_c^2 - \sigma_{nab}\lambda^2)\nabla_\perp$$
$$\times \hat{z}e_z - \frac{1}{c^2}\lambda^2 \frac{\partial^2 \mathbf{b}}{\partial t^2} + \frac{1}{c}(\lambda_c^2 - \lambda^2)\nabla_\perp \times \hat{z}\frac{\partial e_z}{\partial t} \qquad (8)$$

where λ_{ab} has been replaced by λ for convenience. The last two terms on the right-hand side of (8) come from the displacement current and are usually neglected at frequencies no higher than microwave.

In addition to the London electrodynamics described above, we use the hydrodynamic model to describe the flux dynamics. For linear ac response, the linearized hydrodynamic equations are [17]

$$\frac{\partial \delta n}{\partial t} + n_0 \nabla_\perp \cdot \mathbf{v} = 0 \qquad (9)$$

and

$$-\kappa\mathbf{v} + \eta_s \nabla_\perp^2 \mathbf{v} + \eta_b \nabla_\perp(\nabla_\perp \cdot \mathbf{v}) + \eta_z \frac{\partial^2 \mathbf{v}}{\partial z^2} - \frac{1}{c}\mathbf{B}_0 \times \mathbf{j} = 0. \qquad (10)$$

Equation (9) in fact is the equation of continuity for the areal density of vortexes with $\delta n = n - n_0$, the deviation from equilibrium value n_0. Equation (10) is the equation of motion for a moving vortex with velocity v and friction coefficient κ. The coefficients η_s, η_b, and η_z are the shear, bulk, and tilt-viscosity constants, respectively. Based on (8)–(10), one can investigate the ac response of the flux-line liquid provided that magnetic flux density b is found.

An ac field $\mathbf{H}_a = \hat{y}\delta H_a e^{j\omega t}$ is applied parallel to the rectangular rod (also parallel to H) with $\delta H_a \ll H$. The local field b in (8) is assumed to be in the form of $\mathbf{b} = \hat{y}\delta B_y(x, z)e^{j\omega t}$. Besides, the tilt field τ is zero because the flux lines are, on the average, aligned in y-direction. Accordingly, (8) becomes

$$-\lambda_c^2 \frac{\partial^2 \delta B_y}{\partial x^2} - \lambda^2 \frac{\partial^2 \delta B_y}{\partial z^2} + \left(1 + \frac{\lambda^2}{\lambda_{nf}^2}\right)\delta B_y$$
$$= \phi_0 \delta n(x, z) \qquad (11)$$

where $\lambda_{nf} = \sqrt{c^2/j4\pi\omega\sigma_{nab}}$ is the skin depth due to in-plane normal-fluid. In the simple flux-flow dominated-vortex

dynamics, namely in the absence of pinning with $\tilde{\eta}_l = \eta_s + \eta_b = 0$, (11) can be expressed as

$$(\lambda_c^2 + \lambda_f^2)\frac{\partial^2 \delta B_y}{\partial x^2} + (\lambda^2 + \lambda_f^2)\frac{\partial^2 \delta B_y}{\partial z^2}$$

$$- \left(1 + \frac{\lambda^2}{\lambda_{nf}^2}\right)\delta B_y = 0 \qquad (12)$$

where (9) and (10) have been utilized, and $\lambda_f = \sqrt{c_L(0)/j\omega\kappa}$ is the ac penetration length of the flux liquid. Here, $c_L(0)$ is the longitudinal-compressional modulus defined by $c_L(0) = B_0^2/4\pi$ [17]. Equation (12), subject to boundary conditions at $x = \pm a$ and $z = \pm t$, describes a well-defined electrodynamic problem. By letting $x' = x/\sqrt{\lambda_c^2 + \lambda_f^2}$ and $z' = z/\sqrt{\lambda^2 + \lambda_f^2}$, the exact solution for δB_y can be found with the result

$$\delta B_y(x, z) = \sum_{n=0}^{\infty} (-1)^n \frac{2\delta H_a}{q_n}$$

$$\left[\cos\left(\frac{q_n}{a} x\right) \frac{\cosh\left(\frac{z}{\tilde{\lambda}_1}\right)}{\cosh\left(\frac{t}{\tilde{\lambda}_1}\right)} \right.$$

$$\left. + \cos\left(\frac{q_n}{t} z\right) \frac{\cosh\left(\frac{x}{\tilde{\lambda}_2}\right)}{\cosh\left(\frac{a}{\tilde{\lambda}_2}\right)} \right] \qquad (13)$$

where $\tilde{\lambda}_1$ and $\tilde{\lambda}_2$ are given by

$$\tilde{\lambda}_1^{-2} = \frac{1}{\lambda_{nf}^2} \cdot \frac{\lambda^2 + \lambda_{nf}^2}{\lambda^2 + \lambda_f^2} + \frac{q_n^2}{a^2} \cdot \frac{\lambda_c^2 + \lambda_f^2}{\lambda^2 + \lambda_f^2} \qquad (14a)$$

$$\tilde{\lambda}_2^{-2} = \frac{1}{\lambda_{nf}^2} \cdot \frac{\lambda^2 + \lambda_{nf}^2}{\lambda_c^2 + \lambda_f^2} + \frac{q_n^2}{t^2} \cdot \frac{\lambda^2 + \lambda_f^2}{\lambda_c^2 + \lambda_f^2} \qquad (14b)$$

where $q_n = (n + \frac{1}{2})\pi$, $n = 0, 1, 2, 3, \cdots$. The associated dimensionless ac permeability μ is defined by

$$\mu = \frac{1}{2a \cdot 2t \cdot \delta H_a} \int_{-a}^{a} \int_{-t}^{t} \delta B_y(x, z)\, dz\, dx. \qquad (15)$$

After substitution of (13) into (15), one has

$$\mu = \sum_{n=0}^{\infty} \left\{ \frac{2}{q_n^2} \left[\frac{\tanh\left(\frac{t}{\tilde{\lambda}_1}\right)}{\frac{t}{\tilde{\lambda}_1}} + \frac{\tanh\left(\frac{a}{\tilde{\lambda}_2}\right)}{\frac{a}{\tilde{\lambda}_2}} \right] \right\}. \qquad (16)$$

One can also directly calculate the change in the vortex areal density due to ac field penetration from (11). Simple manipulation gives

$$n(x, z) = \phi_0^{-1} \sum_{n=0}^{\infty} (-1)^n \frac{2\delta H_a}{q_n}$$

$$\left[K_1 \cos\left(\frac{q_n}{a} x\right) \frac{\cosh\left(\frac{z}{\tilde{\lambda}_1}\right)}{\cosh\left(\frac{t}{\tilde{\lambda}_1}\right)} \right.$$

$$\left. + K_2 \cos\left(\frac{q_n}{t} z\right) \frac{\cosh\left(\frac{x}{\tilde{\lambda}_2}\right)}{\cosh\left(\frac{a}{\tilde{\lambda}_2}\right)} \right] \qquad (17)$$

where

$$K_1 = 1 + \frac{\lambda^2}{\lambda_{nf}^2} \cdot \frac{\lambda_f^2 - \lambda_{nf}^2}{\lambda^2 + \lambda_f^2}$$

$$+ \left(\frac{q_n}{a}\right)^2 \lambda_f^2 \frac{\lambda_c^2 - \lambda^2}{\lambda^2 + \lambda_f^2} \qquad (18a)$$

and

$$K_2 = 1 + \frac{\lambda^2}{\lambda_{nf}^2} \cdot \frac{\lambda_f^2 - \lambda_{nf}^2 + \lambda_c^2 - \lambda^2}{\lambda_c^2 + \lambda_f^2}$$

$$+ \left(\frac{q_n}{t}\right)^2 \lambda_f^2 \frac{\lambda^2 - \lambda_c^2}{\lambda_c^2 + \lambda_f^2}. \qquad (18b)$$

So far we have calculated the complex ac permeability of the flux-line liquid in the simple flux-flow regime for an anisotropic superconductor in the shape of a rectangular rod in a parallel field. The permeability in (16) is obviously dependent on the sample dimensions and model of flux-line dynamics. In the hydrodynamic model considered here, the permeability is related to the normal-fluid skin depth arising from ab-plane normal electrons and the ac penetration length due to friction together with static viscosity in a flux liquid.

Before we demonstrate the numerical results, some special results from (16) will be discussed in advance. As is customary, the most commonly used geometries for the theoretical study of microwave or ac response in HTSC are the slab and cylinder. Therefore, the reduction to slab limit from (16) is naturally expected. In the limit of $a \to \infty$, (16) can be simplified

$$\mu_{slab} = \frac{\tanh\left(\frac{t}{\tilde{\lambda}_1}\right)}{\frac{t}{\tilde{\lambda}_1}} \qquad (19)$$

where $\tilde{\lambda}_1$ expressed in (14a) is now given by

$$\tilde{\lambda}_1^2 = \frac{\lambda^2 + \lambda_f^2}{1 + \frac{\lambda^2}{\lambda_{nf}^2}} \qquad (20)$$

and

$$\frac{t}{\tilde{\lambda}_1} = \left(\frac{1 + \frac{j\omega}{\omega_{nf}}}{\frac{\lambda^2}{t^2} + \frac{\omega_D}{j\omega}}\right)^{1/2} \qquad (21)$$

where $\omega_D = \lambda^2\omega_f/t^2$ is the inverse of the characteristic time for flux diffusion across the slab. Equation (19) is the permeability for a c-axis-oriented thin slab with a thickness of $2t$ which conveys the anisotropic feature; namely it relies on the ab-plane penetration depth described as λ here. Furthermore, for an isotropic slab, (19)–(21) separately reduce to the results of Chen and Marchetti; see [17, eqs. (3.5), (3.8), (3.10)]. Besides, the ac response for a slab is primarily dominated by

a single ac penetration depth $\tilde{\lambda}_1$ which relies on the magnetic dependence of the *in*-plane London penetration depth λ and ac penetration length of flux liquid λ_f in addition to the normal-fluid skin depth λ_{nf}. As $H \to H_{c2}$, implying a divergent λ, then $\tilde{\lambda}_1 \to \lambda_{nf}$. Accordingly, the permeability reduces to the normal-state response of superconductors. A similar result is also given in the Coffey–Clem model where the ac penetration length $\tilde{\lambda}$ is given by [9]–[11]

$$\tilde{\lambda} = \left[\frac{\lambda^2 + (\lambda_p^{-2} + 2j\delta_f^{-2})^{-1}}{1 + \left(\dfrac{2j\lambda^2}{\delta_{nf}^2}\right)} \right]^{1/2} \quad (22)$$

where $\lambda_p^2 = B_0\phi_0/4\pi\kappa_p$ is the Campbell pinning-penetration depth [22] with pinning constant κ_p, $\delta_f^2 = B_0\phi_0/2\pi\eta\omega$, the flux-flow penetration depth with friction coefficient η, and the normal-fluid skin depth $\delta_{nf}^2 = c^2/(2\pi\omega\sigma_{nab})$. Again, as $H \to H_{c2}$, $\tilde{\lambda} \to \delta_{nf}(1-j)/2 = \lambda_{nf}$, reducing to the normal-state response.

III. NUMERICAL RESULTS AND DISCUSSION

We first consider the simple case, the isotropic-superconducting rectangular rod with anisotropic ratio $\gamma = \lambda_c/\lambda = 1$. In this case, the complex penetration lengths $\tilde{\lambda}_1$ and $\tilde{\lambda}_2$ in (14) reduce to

$$\tilde{\lambda}_1 = \left[\frac{1}{\lambda_{nf}^2} \cdot \frac{\lambda^2 + \lambda_{nf}^2}{\lambda^2 + \lambda_f^2} + \frac{q_n^2}{a^2} \right]^{-1/2} \quad (23a)$$

$$\tilde{\lambda}_2 = \left[\frac{1}{\lambda_{nf}^2} \cdot \frac{\lambda^2 + \lambda_{nf}^2}{\lambda^2 + \lambda_f^2} + \frac{q_n^2}{t^2} \right]^{-1/2} \quad (23b)$$

respectively. Based on (23), the behavior of permeability in (16) can be numerically investigated. In Fig. 1(a), we plot the imaginary part of permeability μ'' as a function of frequency for various thin platelets at fixed thicknesses $t = 10\,\lambda$ and $\omega_{nf}/\omega_f = 50$. Here, the aspect ratio p is defined as $p = a/t$. For $p = 1$, one refers to it as a thin square rod and $p \to \infty$ as the infinite thin slab with thickness $2t$. The infinite thin slab simply describes the field penetration through two main flat surfaces; namely the ac field penetration through thin edges is neglected. Its corresponding permeability is given in (19) and (21). At very low frequencies, $\omega \ll \omega_D$, then $|\tilde{\lambda}_1| \gg t$ from (21) and field penetration is complete, yielding a smaller μ'' and a larger μ' with $\mu' \approx 1$. At intermediate frequencies, $\omega_D \ll \omega \ll \omega_f$, $\tilde{\lambda}_1 \sim t \to \mu \approx \mu' \approx \tanh(t/\lambda)/(t/\lambda) \approx 0.1 \ll 1$. The ac field can solely penetrate a surface layer of width λ, indicating the flux liquid cannot diffuse on the time scale over which the perturbed field changes. The transition [17] from $\mu' \approx 1$ to $\mu' \approx 0.1$ is marked by a dissipation-μ'' peak with a value of about 0.41 as shown in Fig. 1(a). For higher frequency, $\omega \gg \omega_{nf}$, the normal-fluid becomes dominant, leading to $\mu' \sim 0$. The second transition in μ' is accompanied by a second small peak in μ'' with a value of ~ 0.04. The first-μ'' peak occurs at $\log_{10}(\omega/\omega_f) \approx -1.6 \to$

$t/|\tilde{\lambda}_1| \approx 1.61$ which is somewhat greater than the usual skin-size effect $t/|\tilde{\lambda}_1| \approx 1.13$ given by standard descriptions of flux-line dynamics [9], [12], [13]. By reducing the width of the platelet such that $p = a/t = 10, 4, 2, 1$, the field penetration through thin edges is thus included, and the permeability is controlled by $\tilde{\lambda}_1$ and $\tilde{\lambda}_2$ in (23). As shown in Fig. 1(a), the introduction of field absorption from thin edges has lowered the height of the first peak in μ'' from 0.41 (maximum, for slab, $p \to \infty$) to 0.35 (minimum, for square rod, $p = 1$). The change in sample width can vary the size of the μ'' peak by 14.6% below its maximum value in the slab. Also, the frequency in the first-μ'' peak increases with decreasing p. As for the second small peak in μ'', the inclusion of field penetration through thin edge surfaces, however, raises the peak height, and no appreciable change in the peak frequency is observed. In Fig. 1(b), the same condition is illustrated for a much thinner platelet with thickness $t = 2\lambda$. The figure indicates that the thin edge has a salient influence on the ac properties of flux-line liquid. The first peak height in μ'' was depressed considerably and changed from a maximum peak of 0.26 (in the slab) to a minimum one of 0.16 (in the square rod). The variation is now increased up to 38%, greater than that at $t = 10\lambda$. In addition, the second peak is enhanced, especially for the thin square rod, having a maximum peak value of 0.235. The results clearly reveal that the ac absorption from thin edge surfaces cannot be neglected, even in the isotropic superconductor. As argued by Gough *et al.* [4], the losses from thin edges would be usually negligible for an isotropic superconductor. Based on the results shown in Fig. 1, this argument does not appear to be fully correct. One must equally treat the thin edges in the study of a mixed-state ac response of an isotropic superconductor.

As is known, the cylinder is usually considered for theoretical calculation of ac permeability. However, the exact expression of magnetic permeability for an anisotropic cylinder is not available so far. The main difficulty lies in the finding of distribution for the magnetic flux density inside a superconducting cylinder. We therefore pay attention to the ac response of an isotropic cylinder for the time being. An interesting question then arises. Can the ac permeability of an isotropic cylinder be intuitively replaced by a square rod with an equal cross section area and vice versa? The issue will be numerically discussed and answered as follows. The ac-magnetic permeability for an isotropic superconducting cylinder with a radius of ρ is given by [23]

$$\mu_{cy\,\text{in}} = 2\frac{\tilde{\lambda}_1}{\rho} \cdot \frac{I_1\left(\dfrac{\rho}{\tilde{\lambda}_1}\right)}{I_0\left(\dfrac{\rho}{\tilde{\lambda}_1}\right)} \quad (24)$$

where $\tilde{\lambda}_1$ is the same as given in (20); I_0 and I_1 are the Bessel functions of the first kind of orders zero and one, respectively. The imaginary and real parts of permeability of the cylinder [(24) with $\rho = 2\lambda$] are separately depicted in Fig. 2(a) and (b) where the permeabilities of the square rod [(16), (23)] at distinct sizes $a = t = \lambda$, $\sqrt{\pi}\lambda$, and 2λ are also given for the purpose of comparison. It is obvious that the permeability of the cylinder falls between those of square rods at $a = \sqrt{\pi}\lambda$
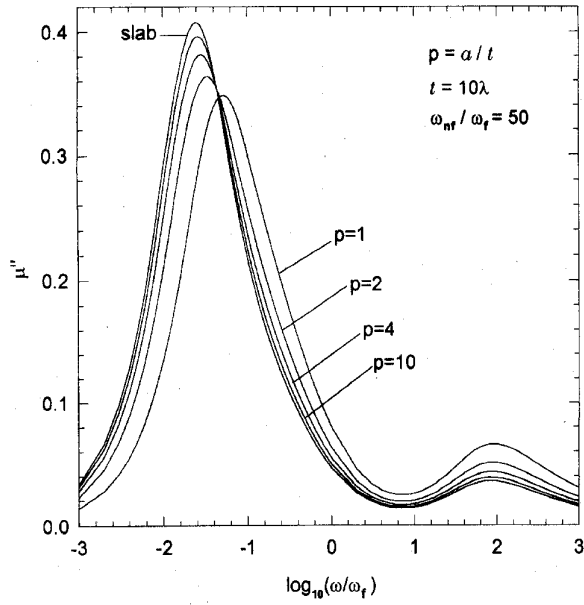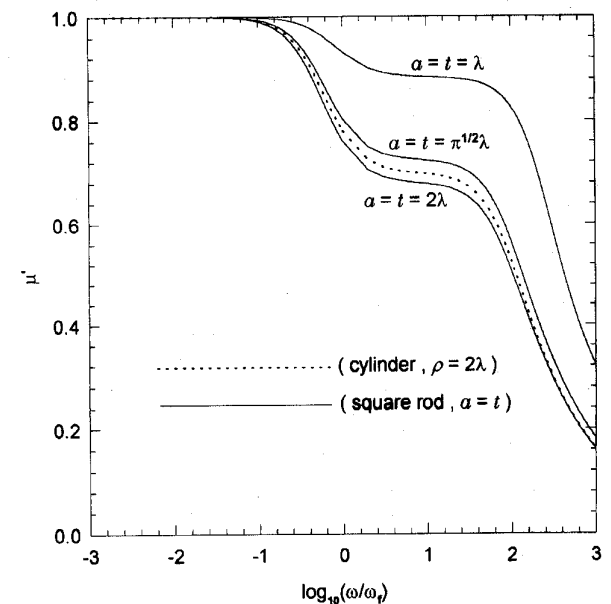
(a)
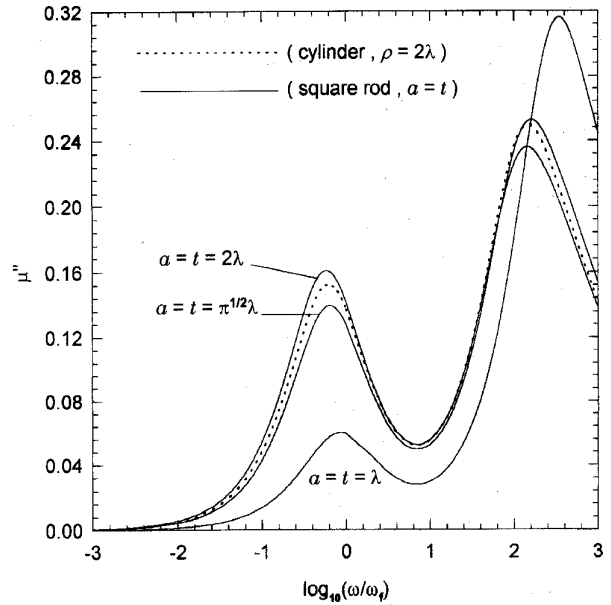
(a)
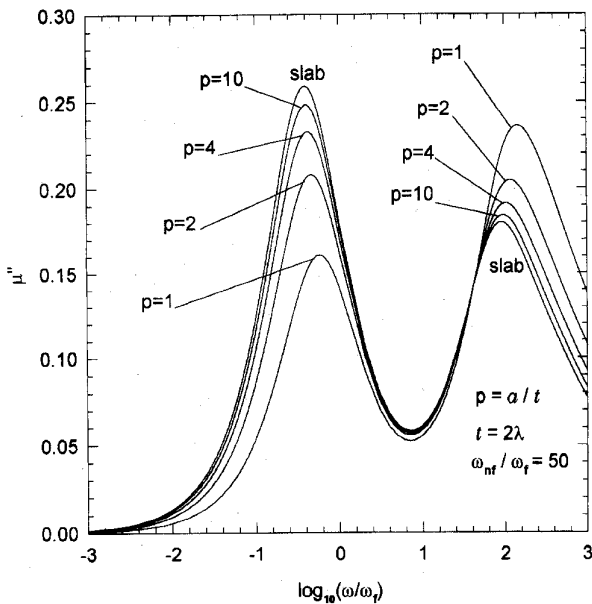
(b)

(b)

Fig. 1. (a) The frequency dependence of imaginary parts of permeabilities in (20) for the slab and (17) for the rectangular rod at various aspect ratios of $p = 1, 2, 4, 10$ and $\omega_{nf}/\omega_f = 50$. (b) The frequency dependence of imaginary parts of permeabilities in (20) for the slab and (17) for the rectangular rod at various aspect ratios of $p = 1, 2, 4, 10$ for $t = 2\lambda$ and $\omega_{nf}/\omega_f = 50$.

Fig. 2. (a) The imaginary part of permeabilities for an isotropic cylinder in (25) and a square rod in (17) at $\omega_{nf}/\omega_f = 50$. The radius of the cylinder is taken to be $\rho = 2\lambda$. (b) The real part of permeabilities for an isotropic cylinder in (25) and a square rod in (17) at $\omega_{nf}/\omega_f = 50$. The radius of the cylinder is taken to be $\rho = 2\lambda$.

and $a = 2\lambda$. Essentially, in the interesting frequency regime, Fig. 2 indicates that the ac permeability of a cylinder can be better approximated by that of a square rod with $a = 2\lambda$. Such approximation implies that both cylinder and square rod do not have an equal cross-section area. The cross-section area ratio of cylinder to square rod is found to be about $\pi/4 \approx 0.785$. The results here suggest that the study of a cylinder's ac response can be replaced, if necessary, by a square rod with a specified width and vice versa.

We go on to investigate the influence of anisotropy on ac response based on (14) and (16). For a thick square rod with $a = t = 10\lambda$, the frequency dependence of the dissipation part at various anisotropic ratios, γ, is shown in Fig. 3(a). The first peak height in μ'' has been lowered considerably with an increase in γ, whereas the second peak height is greatly raised. For $\gamma = 8$, corresponding to the maximum anisotropy in the YBCO system [21], the second peak is greater than the first peak. At $\gamma = 50$, the minimum anisotropic ratio reported in the
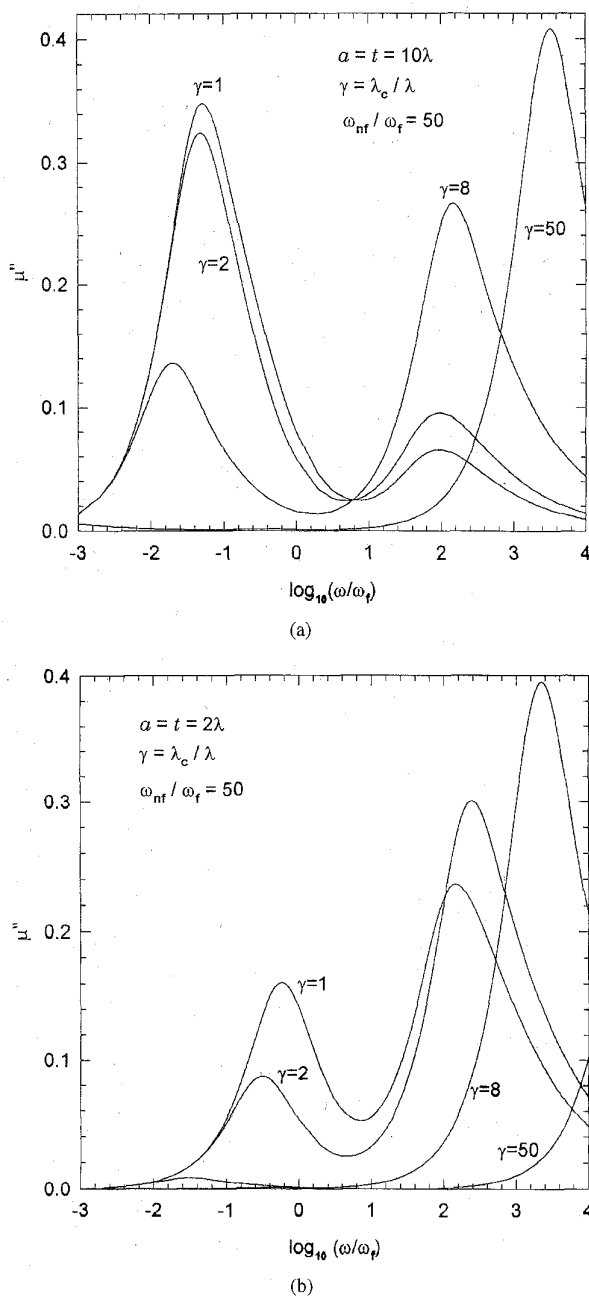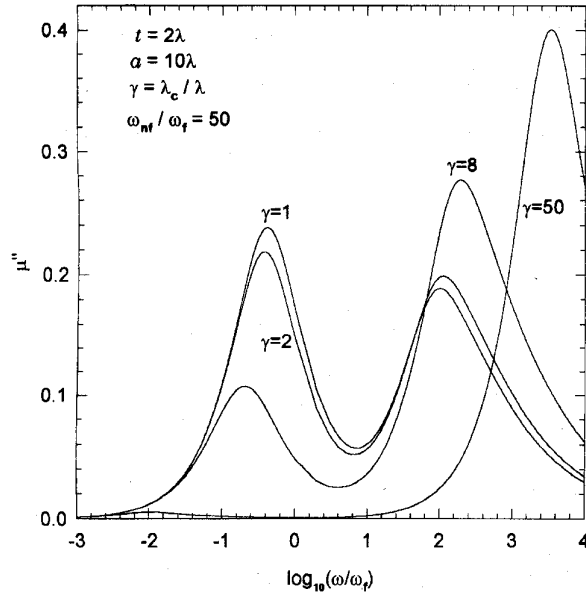
(a)

(b)

Fig. 3. (a) The frequency dependence of the imaginary part of permeability in (17) for an anisotropic square rod at various anisotropic ratios of $\gamma = 1, 2, 8, 50$ for $a = t = 10\lambda$ and $\omega_{nf}/\omega_f = 50$. (b) The frequency dependence of the imaginary part of permeability in (17) for an anisotropic square rod at various anisotropic ratios of $\gamma = 1, 2, 8, 50$ for $a = 10\lambda, t = 2\lambda$, and $\omega_{nf}/\omega_f = 50$.

Bi-based high-T_c system [21]; the first peak in μ'' is obscure, and only the second peak is observed with a large peak value. The same situations for the thin square rod with $a = t = 2\lambda$ are also indicated in Fig. 3(b). It is noteworthy that the first peak in $\gamma = 8$ becomes negligibly small, and the second peak height has effectively increased to ~ 0.4. For a thin rectangular platelet, $t = 2\lambda$ and $a = 10\lambda$, the μ'' is shown in Fig. 4(a). Again, the increase in γ will lower the first dissipation peak and enhance the second loss peak. By comparing with

Fig. 3(a), one would find that the thin edge surfaces have much influence on the permeability in isotropic ($\gamma = 1$) and very weakly anisotropic ($\gamma = 2$) superconductors. As for $\lambda = 8$ and $\gamma = 50$, the only appreciable change is observed in the overall behaviors in μ''. If one compares with Fig. 3(b), the results reveal that the increase in width, a, has a pronounced effect on the ac response of flux-line liquid for both isotropic and anisotropic superconductors. Fig. 4(b) shows the response for the thin platelet ($t = 2\lambda$) with a large width of $a = 100\lambda$. The large width makes the two-peak feature in μ'' visible for both isotropic and anisotropic superconductors. What is more, the increase in γ (more anisotropy) makes the two-peak frequencies change appreciably. Finally, Fig. 5 shows the μ'' for an anisotropic thin platelet ($\gamma = 8, t = 2\lambda$) at various widths of $a = 2\lambda$, 10λ, 50λ, and 100λ. Here, the first peak height increases with increasing width, whereas the size of the second peak decreases with increasing width. The decrease in width implies a heavy ac field penetration through a thin edge surface. Accordingly, the first peak is strongly suppressed while the second peak heavily increases. The first peak height changes from 0.24 (for $a = 100\lambda$, nearly as infinite slab) to 0.01 (for $a = 2\lambda$, square rod). The variation here is almost 95.8%, far greater than 38% given in the isotropic one as shown in Fig. 1(b). In addition, the frequency at the first peak is moved to lower values and the one at the second peak to higher values when the width is reduced, opposite to isotropic results indicated in Fig. 1(b). With a careful look at Fig. 5 as well as Fig. 1(b), one would conclude that the effect of width due to anisotropy is more pronounced than the isotropic ones. Care, therefore, should be taken in the study of ac properties in the anisotropic superconductors. For the single crystal YBCO ($\gamma = 8$) platelet, the sample is usually arranged with a/t much greater than ten, and the two-peak behavior is therefore expected. For the low-frequency regime conducted in the experiment, one would at least observe the first peak in μ''. The above-described results in Figs. 3–5 have unambiguously shown the correlation of permeability with the anisotropy ratio and size of the sample as well.

IV. CONCLUSION

The ac response of flux-line liquid in the flux-flow dynamics in the anisotropic high-temperature superconducting-rectangular platelet has been systematically investigated in this study. Two-peak behavior in the dissipation part of permeability is observed. The two peaks correspond to the two transitions in the real part of ac permeability. The response is essentially divided into three regions via two frequency scales. The two-peak feature is, however, strongly influenced by the sample size and material anisotropy. For fixed thickness in thin edge surfaces, the increase in width increases the size of the first peak and decreases the second peak height in both isotropic and anisotropic superconductors. The influence of a platelet's width is more salient in the anisotropic ones. In an anisotropic thin platelet, the increase in anisotropy lowers the first peak height while the second peak is raised. Furthermore, the shift in peak frequency in anisotropic superconductors is quite contrary to the isotropic one. As for the isotropic square

(a)
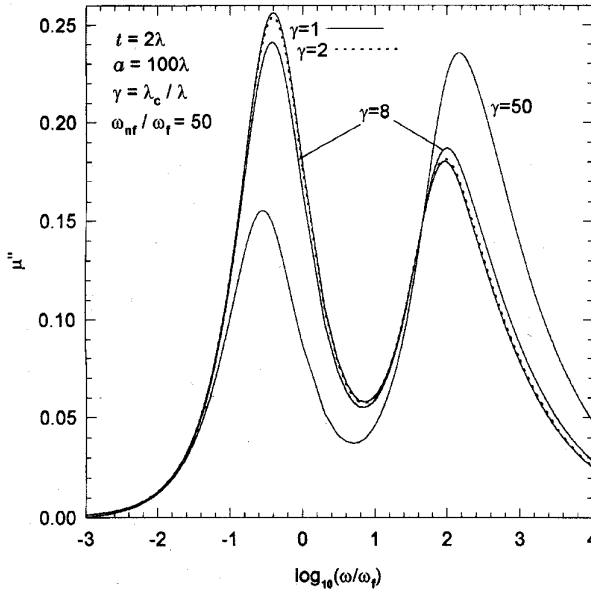
(b)

Fig. 4. (a) The frequency dependence of the imaginary part of permeability in (17) for an anisotropic rectangular platelet at various anisotropic ratios of $\gamma = 1, 2, 8, 50$ for $a = 10\lambda, t = 2\lambda$, and $\omega_{nf}/\omega_f = 50$. (b) The frequency dependence of the imaginary part of permeability in (17) for an anisotropic rectangular platelet at various anisotropic ratios of $\gamma = 1, 2, 8, 50$ for $a = 100\lambda, t = 2\lambda$, and $\omega_{nf}/\omega_f = 50$.

rod, we find its permeability can be approximately replaced by an isotropic cylinder in the same field configuration when the cross section-area ratio of cylinder to square rod is approximately specified by $\pi/4$. The analysis presented here suggests the dependence of flux-line dynamics on material anisotropy and sample dimensions, rarely investigated so far. The present results provide much fundamental information which is of particular importance in the study of ac properties of a flux-line system.
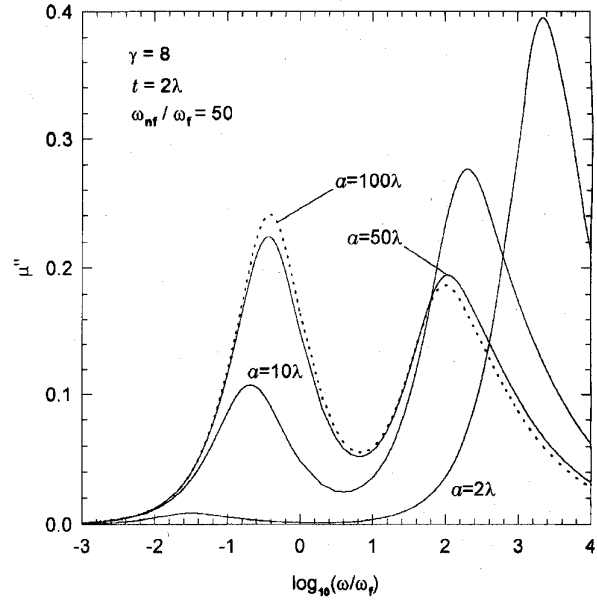

Fig. 5. The frequency dependence of the imaginary part of permeability in (17) for an anisotropic rectangular platelet at various widths of $a = 2\lambda, 10\lambda$, $50\lambda, 100\lambda$ for $t = 2\lambda$, $\gamma = 8$, and $\omega_{nf}/\omega_f = 50$.

REFERENCES

[1] J. Owlaiaei, S. Sridhar, and J. Tavlvacchio, "Field-dependence crossover in the vortex response at microwave frequencies in $YBa_2Cu_3O_{7-x}$ films," *Phys. Rev. Lett.*, vol. 69, no. 23, pp. 3366–3369, 1992.

[2] M. S. Pambianchi, D. H. Wu, L. Ganapathi, and S. Anlage, "DC magnetic dependence of the surface impedance in superconducting parallel transmission line resonators," *IEEE Trans. Appl. Supercond.*, vol. 3, no. 1, pp. 2774–2777, 1993.

[3] S. Revenaz, D. E. Oates, G. Dresselhaus, and M. S. Dresselhaus, "Frequency dependence of the microwave surface impedance of $YBa_2Cu_3O_{7-x}$ thin film in a dc magnetic field: Investigation of vortex dynamics," *Phys. Rev. B, Condens. Matter*, vol. 50, no. 2, pp. 1178–1189, 1994.

[4] C. E. Gough and N. J. Exon, "Microwave response of anisotropic high-temperature-superconductor crystals," *Phys. Rev. B, Condens. Matter*, vol. 50, no. 1, pp. 488–495, 1994.

[5] P. P. Nguyen, D. E. Oates, G. Dresselhaus, M. S. Dressellaus, and A. C. Anderson, "Microwave hysteretic losses in $YBa_2Cu_3O_{7-x}$ and NbN thin films," *Phys. Rev. B, Condens. Matter*, vol. 51, no. 10, pp. 6686–6695, 1995.

[6] N. Belk, D. E. Oates, D. A. Feld, G. Dresselhaus, and M. S. Dresselhaus, "Frequency and temperature dependence of the microwave surface impedance of $YBa_2Cu_3O_{7-x}$ thin film in a dc magnetic field: Investigation of vortex dynamics," *Phys. Rev. B, Condens. Matter*, vol. 53, no. 6, pp. 3459–3470, 1996.

[7] S. de Brion, R. Calemczuk, and J. Y. Henery, "Flux line dynamics in crystal $YBa_2Cu_3O_{7-x}$ studied by mechanical measurements," *Physica C*, vol. 178, nos. 1–3, pp. 225–230, 1991.

[8] P. Seng, R. Gross, U. Baier, M. Rupp, D. Koelle, R. P. Huebener, P. Schmitt, G. Saemann-Ischenko, and L.Schultz, "Dissipation flux motion in epitaxial $YBa_2Cu_3O_{7-x}$ and $Bi_2Sr_2CaCu_2O_{8+x}$ films," *Physica C*, vol. 192, nos. 3–4, pp. 403–418, 1992.

[9] M. W. Coffey and J. R. Clem, "Unified theory of effects of vortex pinning and flux creep upon the RF surface impedance of type-II superconductors," *Phys. Rev. Lett.*, vol. 67, no. 3, pp. 386–389, 1991.

[10] _____, "Theory of rf magnetic permeability of type-II superconductors in slab geometry with an oblique static magnetic field," *Phys. Rev. B, Condens. Matter*, vol. 45, no. 18, pp. 10527–10535, 1992.

[11] _____, "Theory of high-frequency linear response of isotropic type-II superconductors in the mixed-state," *Phys. Rev. B, Condens. Matter*, vol. 46, no. 18, pp. 11757–11764, 1992.

[12] E. H. Brandt, "Penetration of magnetic fields into type-II superconductors," *Phys. Rev. Lett.*, vol. 67, no. 16, pp. 2219–2222, 1991.

[13] V. B. Geshkenbein, V. M. Vinokur, and R. Fehrenbacher, "AC absorption in the high-T_c superconductors: Reinterpretation of the irreversibility line," *Phys. Rev. B, Condens. Matter,* vol. 43, no. 4, pp. 3748–3751, 1991.

[14] Y. B. Kim, M. J. Stephen, and W. F. Vinen, *Superconductivty,* R. D. Park, Ed. New York: Marcel Dekker, vol. 2, 1969.

[15] C. J. van der Beek and P. H. Kes, "Dislocation-mediated flux creep in $Bi_2Sr_2CaCu_2O_{8+x}$," *Phys. Rev. B, Condens. Matter,* vol. 43, no. 16, pp. 13032–13041, 1991.

[16] N. C. Yeh, "High-frequency vortex dynamics and dissipation of high-temperature superconductors," *Phys. Rev. B, Condens. Matter,* vol. 43, no. 1, pp. 523–531, 1991.

[17] L. W. Chen and M. C. Maretti, "AC response of the flux-line liquid in high-T_c superconductors," *Phys. Rev. B, Condens. Matter,* vol. 50, no. 9, pp. 6382–6393, 1994.

[18] S. Martin, A. T. Fiory, R. M. Fleming, L. F. Schneemeyer, and J. V. Waszczak, "Temperature dependence of the resistivity tensor in superconducting $Bi_2Sr_2CaCu_2O_8$ crystals," *Phys. Rev. Lett.,* vol. 60, no. 21, pp. 2194–2197, 1988.

[19] R. Busch, G. Ries, H. Werthner, G. Kreiselmeyer, and G. Saemann-Ischenko, "New aspect of the mixed state from six-terminal measurements on $Bi_2Sr_2CaCu_2O_8$ single crystals," *Phys. Rev. Lett.,* vol. 69, no. 3, pp. 522–525, 1992.

[20] T. T. M. Palstra, B. Batlogg, R. B. van Dover, L. F. Schneemeyer, and J. V. Waszczak, "Dissipation flux motion in high-temperature superconductors," *Phys. Rev. B, Condens. Matter,* vol. 41, no. 10, pp. 6621–6632, 1991.

[21] G. Blatter, M. V. Feigelman, V. B. Geshkenbein, A. I. Larkin, and V. M. Vinokur, "Vortices in high-temperature superconductors," *Rev. Mod. Phys.,* vol. 66, no. 21, 1994.

[22] A. M. Campbell and J. E. Events, *Critical Currents in Superconductors.* New York: Barnes & Noble, 1972.

[23] C. J. Wu and T. Y. Tseng, "AC response of vortex liquid in the high-temperature superconducting cylinder," *Physica C,* vol. 260, nos. 1–2, pp. 8–18, 1996.
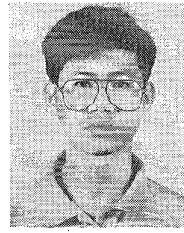
Chien-Jang Wu was born in Taiwan, R.O.C., on March 1, 1962. He received the B.S. degree in electronics engineering, the M.S. degree in electrooptic engineering, and the Ph.D. degree in electronics from National Chiao-Tung University (NCTU), Hsinchu, Taiwan, in 1985, 1990, and 1996, respectively.

Currently, he is working as a Post Doctoral Researcher at National Sun-Yat-Sen University, Physics Department, Kaohsiung, Taiwan. He was an LCD Design Engineer at SEIKO EPSON (Taiwan Branch) from 1990 to 1991. He was also a Telecommunication Hardware Engineer at TranSystem Inc., Hsinchu, Taiwan, from 1991 to 1992. His research interests are in electromagnetic and microwave theory, vortex dynamics, and ac losses of superconductors.

Tseung-Yuen Tseng (M'94–SM'94) received the Ph.D. degree in electroceramics from the School of Materials Engineering at Purdue University, West Lafayette, IN, in 1982.

He was briefly associated with the University of Florida before joining National Chiao-Tung University, Hsinchu, Taiwan, R.O.C., in 1983 where he is now a Professor in the Department of Electronics Engineering and the Institute of Electronics. His professional interests are electronic ceramics, ceramic sensors, and high-temperature ceramic superconductors. He has published more than 110 peer-reviewed technical papers and given 50 conference presentations.

Dr. Tseng was selected for inclusion in *Marquis Who's Who in the World* in 1996 and is a member of the American Ceramic Society. In 1995, he received a distinguished research award from the National Science Council of R.O.C.